Outdoor Urban Propagation Experiment of a Handset MIMO Antenna with a Human Phantom located in a Browsing Stance

Yamamoto, Atsushi; Hayashi, Toshiteru; Ogawa, Koichi; Olesen, Kim; Nielsen, Jesper Ødum; Zheng, Naizheng; Pedersen, Gert Frølund

Published in:
IEEE 66th Vehicular Technology Conference, 2007. VTC-2007 Fall. 2007

DOI (link to publication from Publisher):
10.1109/VETECF.2007.186

Publication date:
2007

Document Version
Publisher's PDF, also known as Version of record

Outdoor Urban Propagation Experiment of a Handset MIMO Antenna with a Human Phantom located in a Browsing Stance

Atsushi Yamamoto, Toshiteru Hayashi, and Koichi Ogawa
Matsushita Electric Industrial Co., Ltd.
1006, Kadoma, Osaka, 571-8501 Japan
{yamamoto.on, hayashi.toshiteru, ogawa.koichi}@jp.panasonic.com

Kim Olesen, Jesper Ø. Nielsen, Naizheng Zheng, and Gert F. Pedersen
Department of Electronic Systems
Aalborg University
Aalborg, Denmark
{ko, jni, nz, gfp}@es.aau.dk

***Abstract*— Outdoor radio propagation experiments are presented at 2.4 GHz, using a handset MIMO antenna with two monopoles and two planar inverted-F antennas (PIFAs), adjacent to a human phantom in browsing stance. The propagation test was performed in an urban area of a city, which resulted in non line-of-sight (NLOS) situations. In our investigation, the 4-by-4 MIMO and SISO channel capacities for the reception signals were evaluated. These measurements show that the handset MIMO antenna, close to the human operator, is capable of MIMO reception.**

Keywords-component; MIMO, Handset antenna, Human phantom, Radio propagation experiment, browsing

I. INTRODUCTION

There have been various investigations into MIMO antenna arrays for application in the handsets used in mobile communications [1]-[4]. Previous studies have shown that MIMO antenna arrays are capable of increasing channel capacities in a multi-path environment in both line-of-sight (LOS) and non line-of-sight (NLOS) cases. However, almost all the investigations have been carried out using calculations and measurements in an anechoic chamber or a simple room [1]-[3]. In reference [5], the MIMO reception characteristics in an urban area in Japan have been examined. However, the array used for the MIMO receiving antenna was only a dipole. Thus, there has been little work to investigate MIMO performance of a mobile handset in realistic situations, with a human operator [4]. In reference [4], however, the investigations were carried out in an outdoor-to-indoor environment and limited to 3-by-4 MIMO. Furthermore, three distributed transmitters with single antennas surrounded the handset.

This paper reports on the performance of a MIMO antenna for a cellular phone, with a human operator. Outdoor radio propagation experiments, using a handset MIMO antenna at 2.4 GHz with a human phantom, were performed in an urban area of a city, resulting in non line-of-sight (NLOS) situations. The handset MIMO antenna consisted of two monopoles and two planar inverted-F antennas (PIFAs), thus permitting the examination of 8-by-4 MIMO reception characteristics. The channel capacity of the MIMO propagation channel was evaluated. The measurements show that the handset MIMO antenna, close to a phantom, provides good MIMO reception.

II. EXPERIMENTAL SETUP

Fig. 1 illustrates the outdoor MIMO propagation test. In the experiment, the handset MIMO antenna, held by a human phantom, was moved on a car trailer. The MIMO channels were collected by a channel sounder [6], [7] inside the car. The sample separation was approximately 1.7 cm, corresponding to 0.14 wavelengths. The handset MIMO was 1.52 m in height from the ground. The antenna array for the base station was mounted on an elevator to be positioned at height of 14.5 m. The array for the base station consisted of eight elements, located linearly. This array was divided into two sub-arrays. Each sub-array had four elements with an element spacing of either one or two wavelengths. In this paper, propagation characteristics of the sub-array with spacing with two wavelengths were evaluated. Spacing between the elements was two wavelengths at 2.4 GHz. Each antenna element had a peak gain of 16.5 dBi and half-power beam-width of 6 degrees in the vertical plane and 85 degrees in the horizontal plane. A vertically polarized wave at 2.4 GHz was transmitted with a power of 34 dBm from each element.

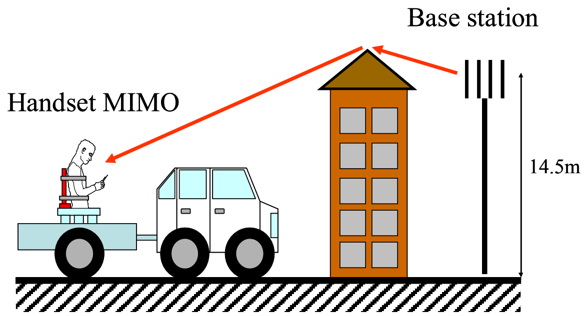

Fig. 1 Outdoor MIMO propagation test.

Fig. 2 depicts the test route in an urban area of Aalborg in Denmark. The route was selected to obtain non line-of-sight (NLOS) situations where the heights of most surrounding building are more than 15 m. The length of the route is about 140 m on the long side of the rectangle route and 100 m on the short side. The propagation characteristics were measured along four sub-routes in straight lines.

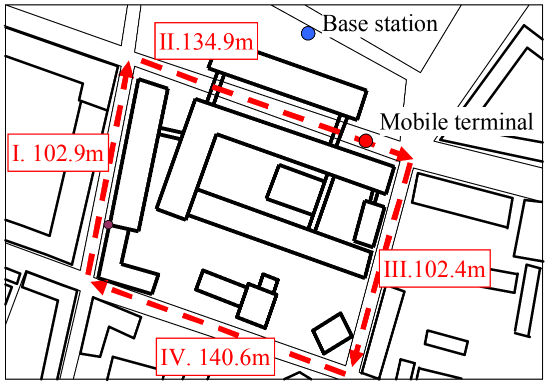

Fig. 2 Test route in an urban area.

III. Handset MIMO Antenna

Fig. 3 illustrates the configuration of the handset MIMO antenna [2] used for our experiment. The handset antenna was comprised of two monopoles and two PIFAs. This antenna enabled us to examine up to 8-by-4 MIMO reception characteristics.

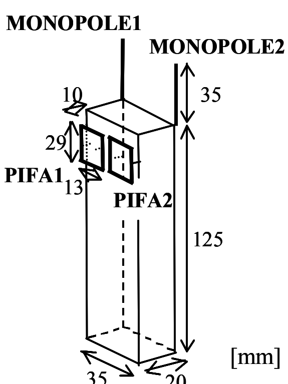

Fig. 3 Configuration of the handset MIMO antenna.

Fig. 4(a) shows the human phantom [8]. The phantom simulated a human operator in a browsing stance, to use the Internet, E-mail, games, etc. The dimensions of the phantom were based on a a standard Japanese adult man. In the outdoor experiment, the handset was held in the right hand of the phantom. The distance, *D,* between the handset and the chest of the phantom was set at 20 cm, and the handset was inclined at angle of 40 degrees from the vertical. Fig. 4(b) shows the handset in free space. This handset was also inclined at angle of 40 degrees from the vertical.

Figs. 5 and 6 show the three-dimensional radiation patterns of the handset MIMO antenna, adjacent to the phantom. In this paper, only the radiation patterns for the monopole 1 and the PIFA 1 are depicted in Figs. 5 and 6, respectively.

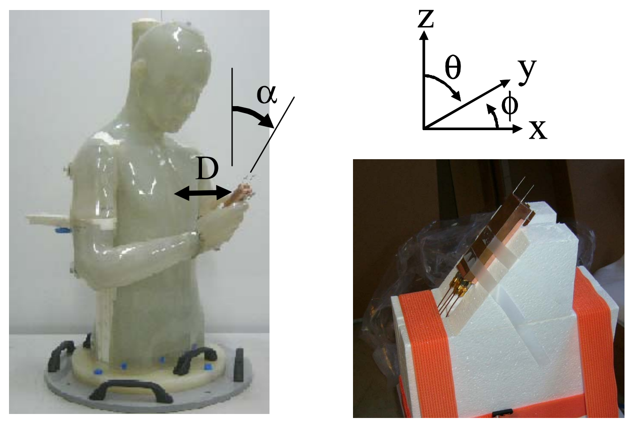

(a) (b)

Fig. 4 Handset situations with.
(a) a human phantom and (b) in free space

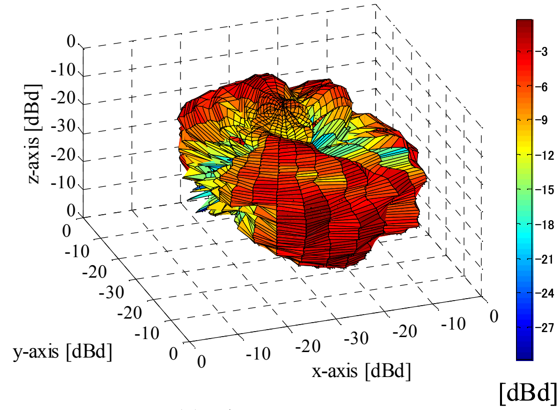

(a) Theta component

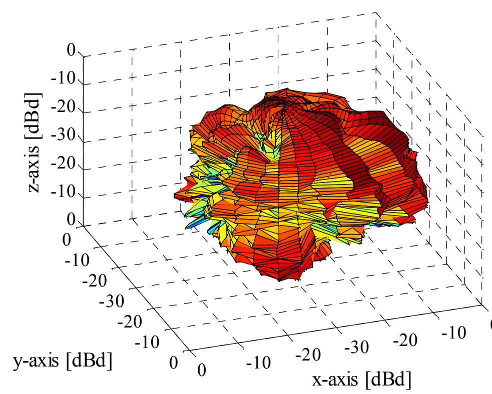

(b) Phi component

Fig. 5 Radiation patterns for the monopole 1 with the phantom.

It may be seen from Figs. 5 and 6 that each antenna radiates strongly in the right hand region of the figures, because the phantom acts as a reflector and both the monopole and PIFA can emit both the theta and phi components. Table 1 lists the radiation efficiencies, η , of each element of the MIMO array with the phantom. As can be seen from Table 1, the radiation efficiencies of the PIFAs are smaller than those of the monopoles, since the PIFAs are located near to the hand of the phantom and are affected by the hand. Furthermore, the PIFA

2 possesses a little worse efficiency than PIFA 1, because of the close proximity of the finger of the phantom.

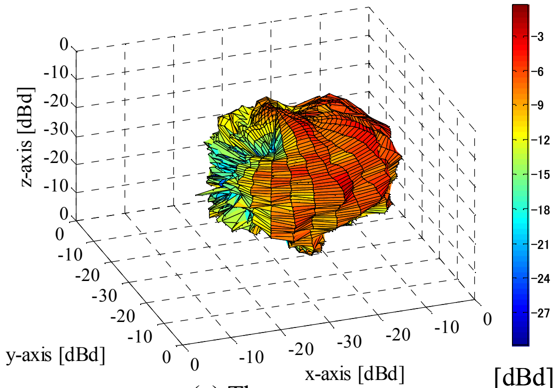

(a) Theta component

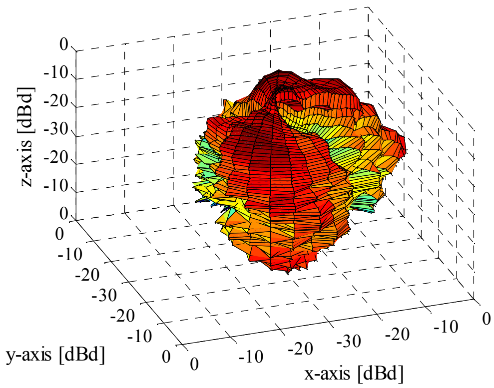

(b) Phi component

Fig. 6 Radiation patterns of the PIFA 1 with the phantom.

Table 1 Radiation efficiencies η of the array in dB.

	Monopole1	Monopole 2	PIFA 1	PIFA 2
η [dB]	-1.2	-1.2	-2.9	-4.3

IV. OUTDOOR MIMO PROPAGATION EXPERIMENT

For this paper, we evaluated the results along the route labeled II. Fig. 7 provides a plot of the variations of the average channel gains of a dipole with a vertical polarization and a slot dipole with a horizontal polarization in free space, when a signal was radiated from only one of the base station antennas Tx1. In this investigation, the data was averaged over 100 samples. Both of the antennas exhibit omni-directional radiation patterns in the horizontal plane. From Fig. 7, the cross polarization discrimination (XPD) of the test site was 9.3 dB. Fig. 8 shows the cumulative distributions of the channel gains of the dipole and slot dipole. Fig. 8 indicates that the channel gains of each antenna were in good agreement with the Rayleigh distribution.

Fig. 9 shows the variations of the average channel gains for the handset MIMO with the phantom. Fig. 10 shows the cumulative distributions of the channel gains, where the mean values, normalized to the free-space dipole data, are listed in Table 2. It is observed from Figs. 9 and 10 that the variations of the channel gains follow the Rayleigh distribution. This indicates that, although the antennas have strong radiations in front of the phantom, a multipath environment needed for a good MIMO performance, was obtained. Furthermore, it is found from Table 2 that the differences in the mean channel gains of the same receiving antenna for different transmitters are small, and that the mean channel gains of the PIFA 2 are the smallest, as also is the radiation efficiency.

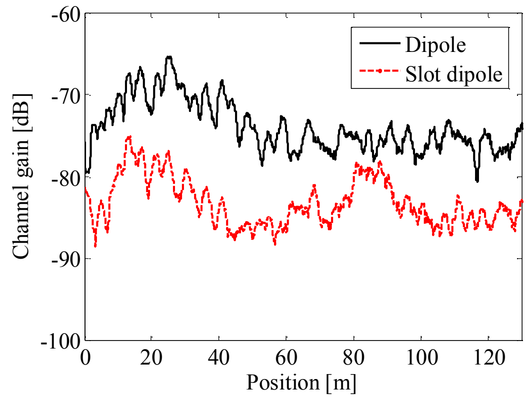

Fig. 7 Variations in the average channel gains of a dipole and a slot dipole when only Tx1 radiated a signal.

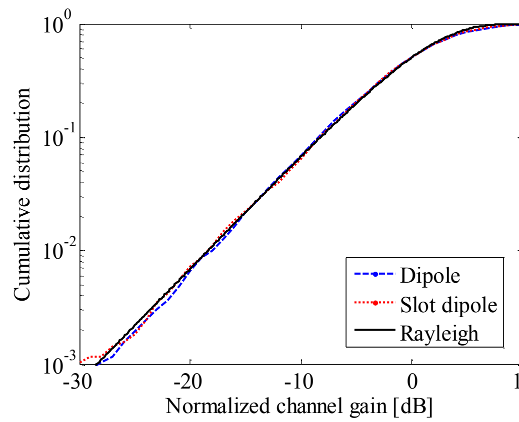

Fig. 8 Cumulative distributions of the channel gains of the dipole and the slot dipole when only Tx1 radiated a signal.

Table 2 Mean values of the channel gains of the handset with the phantom in dB, normalized to that of the free-space dipole.

	Monopole1	Monopole2	PIFA1	PIFA2
Tx1	-2.8	-1.4	-6.0	-7.1
Tx2	-1.9	-0.3	-5.9	-6.8
Tx3	-3.7	-2.0	-7.2	-7.6
Tx4	-3.3	-1.8	-6.9	-7.0

Mean values of the channel gains of the handset MIMO in free space are listed in Table 3. It is found from Tables 2 and 3 that the channel gains in free space are smaller than those with the phantom. Most of the significant path occurs in the front and back of the phantom, since the route II acts as a waveguide between the buildings. Consequently, the handset close to the phantom, with a strong directivity in front of the phantom, can experience stronger reception than it would in free space.

Table 3 Mean values of the channel gains of the handset in free space in dB, normalized to that of the free-space dipole.

	Monopole1	Monopole2	PIFA1	PIFA2
Tx1	-3.5	-2.5	-8.0	-7.9
Tx2	-2.9	-1.8	-7.7	-7.3
Tx3	-3.6	-2.5	-8.1	-6.8
Tx4	-3.5	-2.5	-7.9	-6.6

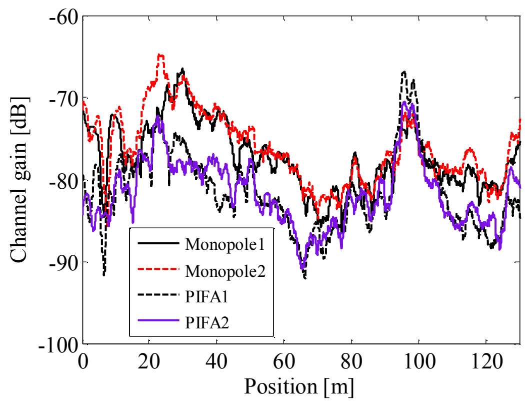

Fig. 9 Variations of the average channel gains of the handset MIMO with the phantom, when only Tx1 radiated a signal.

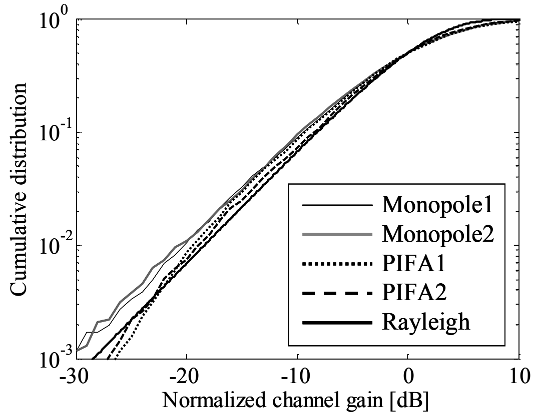

Fig. 10 Cumulative distributions of the channel gains of the handset MIMO with the phantom, when only Tx1 radiated a signal.

Table 4 Fading correlations of the received signals of the handset MIMO with the phantom, when only Tx1 radiated a signal.

	Monopole1	Monopole2	PIFA1	PIFA2
Monopole1	1.0	0.5	0.2	0.3
Monopole2	0.5	1.0	0.2	0.4
PIFA1	0.2	0.2	1.0	0.6
PIFA2	0.3	0.4	0.6	1.0

Table 4 indicates the fading correlations between the received signals of each antenna pair, when only Tx1 radiated a signal. It is observed from Table 4 that the MIMO antenna exhibits low correlations, from 0.2 to 0.6. These low correlations suggest that a good MIMO reception performance might be provided, even though the handset was held by the phantom. Furthermore, the fading correlations in free space are listed in Table 5. It is found from Tables 4 and 5 that the phantom does not degrade the correlations of the MIMO array.

Table 5 Fading correlations of the received signals of the handset MIMO in free space, when only Tx1 radiated a signal.

	Monopole1	Monopole2	PIFA1	PIFA2
Monopole1	1.0	0.4	0.4	0.3
Monopole2	0.4	1.0	0.3	0.5
PIFA1	0.4	0.3	1.0	0.4
PIFA2	0.3	0.5	0.4	1.0

Fig. 11 shows the cumulative distributions of the eigenvalues of the handset MIMO with the phantom, calculated from the channel gains. From Fig. 11, the difference between the first and forth eigenvalues is somewhat small. It can thus be predicted that the MIMO reception can be utilized when the MIMO array is held by the phantom.

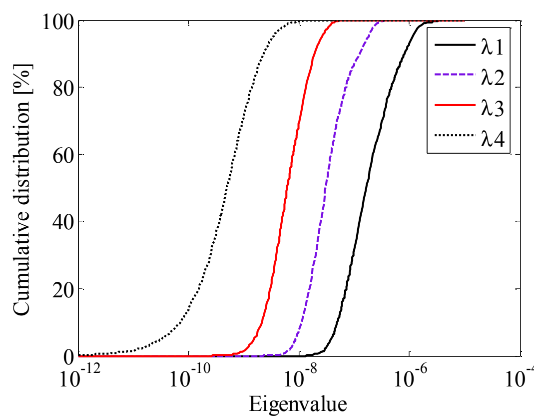

Fig. 11 Cumulative distributions of the eigenvalues of the handset MIMO with the phantom.

Fig. 12 shows the variations of the average channel capacities of a SISO and MIMO with the phantom. Cumulative distributions are shown in Fig. 13. In the calculation, the SNR was normalized to the SNR of a dipole in free space. The SNR of the dipole was set at 15 dB. The mean values of the channel capacities with the phantom are summarized in Table 6. From Figs. 12 and 13, and Table 6, the MIMO channel capacity of the handset achieves a factor of four more than the SISO capacity. This indicates that a good MIMO performance of the handset MIMO could be successfully obtained when the handset was held by the phantom.

Fig. 14 provides comparison between the cumulative distributions of the channel capacities of the MIMO including the phantom and in free space. The average channel capacity of the MIMO in free space is listed in Table 6. As can be seen from Fig. 14 and Table 6, there is little difference between the channel capacities of the MIMO in the two cases.

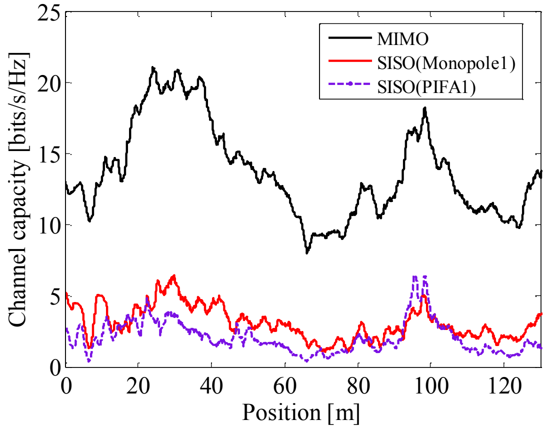

Fig. 12 Variations in the average channel capacities of a SISO and MIMO with the phantom.

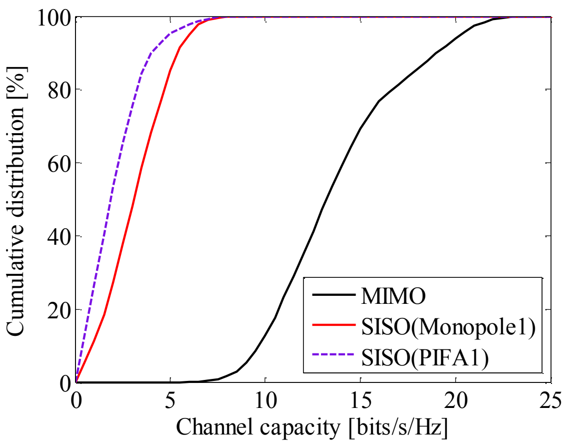

Fig. 13 Cumulative distributions of the channel capacities of a SISO and MIMO with the phantom.

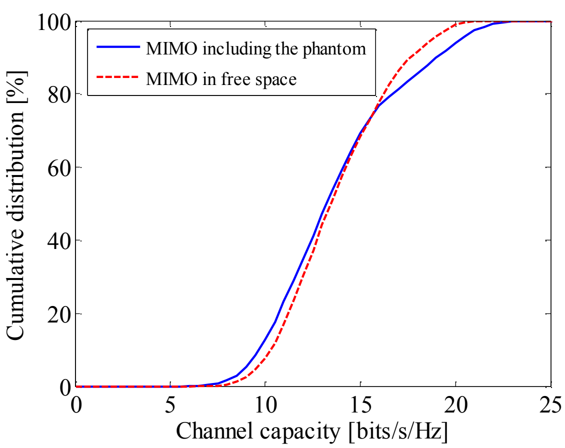

Fig. 14 Comparison between the CDFs of the channel capacities of the MIMO including the phantom and in free space.

We conclude from the outdoor MIMO radio propagation test in the urban NLOS situation that handset MIMO antennas, close to a human operator in the browsing stance can provide good MIMO reception characteristics, and no capacity reduction due to the phantom was found.

Table 6 Average channel capacities, in bits/s/Hz, of a SISO, a MIMO with the phantom, and MIMO in free space.

Phantom			Free space
MIMO	Monopole1	PIFA1	MIMO
13.7	3.2	2.1	13.7

V. Conclusion

Outdoor radio propagation experiments with a Handset MIMO antenna at 2.4 GHz, with a human phantom in browsing stance, were performed in an urban area of a city, resulting in non line-of-sight (NLOS) situations. The channel capacity characteristics of a 4-by-4 MIMO propagation channel were evaluated. These measurements show that the handset MIMO antenna close to the phantom is capable of good MIMO reception.

We have also examined MIMO characteristics of four other handsets with the other two types of phantom. Comparisons of other combinations of handsets and phantoms will be made in future.

References

[1] K. Ogawa, H. Iwai, A. Yamamoto, and J. Takada, "Channel capacity of a handset MIMO antenna influenced by the effects of 3D angular spectrum, polarization, and operator," APS 2006, Albuquerque, USA, pp. 153 - 156, July 2006.

[2] H. T. Hui, "Practical dual-helical antenna array for diversity/MIMO receiving antennas on mobile handsets," *IEE Proc.-Microw. Antennas Propag*., Vol. 152, No. 5, pp. 367 - 372,October 2005.

[3] M. C. Mtumbuka, and D. J. Edwards, "Investigation of tri-polarised MIMO technique," *IEEE ELECTRONICS LETTERS* Vol. 41 No. 3, pp. 137 - 138, Feb. 2005.

[4] W. A. T. Kotterman, G. F. Pedersen, and K. Olesen, "Capacity of the mobile MIMO channel for a small wireless handset and user influence," PIMRC 2002, Lisboa, Portugal, vol.4, pp. 1937 – 1941, Sept. 2002.

[5] K. Nishimori, Y. Makise, M. Ida, R. Kudo, and K. Tsunekawa, "Channel Capacity Measurement of 8 x 2 MIMO Transmission by Antenna Configurations in an Actual Cellular Environment," *IEEE Trans. Antennas Propagat.*, vol. 54, no. 11, pp. 3285 – 3291, Nov. 2006.

[6] J. Ø. Nielsen, J. B. Andersen, P. C. F. Eggers, G. F. Pedersen, K. Olesen, E. H. Sørensen, H. Suda, "Measurements of Indoor 16×32 Wideband MIMO Channels at 5.8 GHz," ISSSTA 2004, Sydney, Australia, pp. 864 - 868, Aug. 2004.

[7] J. Ø. Nielsen and J. B. Andersen, "Indoor MIMO channel measurement and modeling," WPMC'05, Aalborg, Denmark, pp. 479–483, Sep. 2005.

[8] K. Ogawa, H. Iwai, and N. Hatakenaka, "3D-radiation measurements of a handset diversity antenna close to a realistic human phantom in a PDA situation," APS 2003, Columbus, USA, vol. 2, pp. 1029 - 1032, June 2003